



Published in final edited form as:

*Langmuir*. 2011 April 5; 27(7): 3803–3807. doi:10.1021/la2000206.

## Steering Cell Migration Using Microarray Amplification of Natural Directional Persistence

**Girish Kumar, Carlos C. Co, and Chia-Chi Ho**

Chemical & Materials Engineering Department, University of Cincinnati, Cincinnati, OH, USA  
45221-0012

### Abstract

Cell locomotion plays key roles in embryonic morphogenesis, wound healing, and cancer metastasis. Here we show that intermittent control of cell shape using microarrays can be used to amplify the natural directional persistence of cells and guide their continuous migration along preset paths and directions. Key to this geometry-based, gradient-free approach for directing cell migration is the finding that cell polarization, induced by the asymmetric shape of individual microarray islands, is retained as cells traverse between islands. Altering the intracellular signals involved in lamellipodia extension (Rac1), contractility (RhoA), and cell polarity (Cdc42) alters the speed of fibroblast migration on these micropatterns, but does not affect their directional bias significantly. These results provide insights on the role of cell morphology in directional movement and the design of micropatterned materials for steering cellular traffic.

### Introduction

Cell migration is a complex process requiring dynamic coordination of cytoskeletal activity with membrane protrusion and adhesion systems. Upon encountering external stimuli, mammalian cells polarize into a “front” forward moving portion and a “rear” retracting portion that are defined by distinct signaling events.<sup>1</sup> Changes in cellular architecture, such as the re-organization of the microtubule-organizing centre (MTOC), microtubules and Golgi apparatus to the front of the nucleus, accompany polarization. The first step of cell migration is driven by actin polymerization which lead to directional protrusion of lamellipodia in the leading edge.<sup>2,3</sup> The second step is formation of new adhesions in front. Actin-myosin based contraction<sup>4</sup> or its direct transport<sup>5,6</sup> generates traction to move cells forward. The last step in locomotion comprises detachment and retracting the rear.

By culturing cells on microfabricated ECM islands with defined geometry on the micrometer scale, the direction in which cells extend new lamellipodia, filipodia and microspikes can be influenced by the global shape of the cell.<sup>7,8</sup> We and others have also demonstrated that by positioning microarrays asymmetrically,<sup>9,10</sup> micropatterns can be used to guide directional cell motility without any external gradient. However, directional migration in these earlier reports arises from both morphological polarization and availability of adhesive island in front or on the side for lamellipodia attachment. In fact, it was shown that the asymmetric positioning of islands, which determines the availability of adhesive islands for lamellipodia attachment, can overcome any directional bias arising from the shape of the individual teardrop-shaped islands. Here we show that morphological polarization imposed by the adhesive island alone is retained as cells traverse across islands

Address correspondence to: Chia-Chi Ho, Ph.D, Department of Chemical and Materials Engineering, University of Cincinnati, 497 Rhodes Hall, Phone: (513) 5562731, Fax: (513) 5563473.

and thus sufficient to guide continuous directional cell migration. This positive result led us to examine further if directional motility on these micropatterns is retained for cells with varying level of RhoGTPases involved in lamellipodia extension, contractility, and cell polarity.

## Experimental Section

Tissue culture dishes were purchased from Fisher Scientific (Catalog No. 430166) and used as received. Polydimethylsiloxane (PDMS; Sylgard 184) was obtained from Dow Corning (Midland, MI). Random copolymers of oligoethyleneglycol methacrylate and methacrylic acid poly(OEGMA-co-MA) with OEGMA:MA weight ratio of 80:20 were prepared following the procedure described earlier.<sup>11</sup> Alexa 488-phalloidin, 4',6-diamidino-2-phenylindole (DAPI), were purchased from Molecular Probes (Eugene, OR). Phosphate buffer saline was purchased from Sigma (St. Louis, MO). Opti-MEM<sup>®</sup> media was purchased from invitrogen, Serum Supreme, were purchased from Cambrex biosciences (Walkersville, MD).

Micropatterns consisting of different geometric shapes like squares, circles, ellipse and rectangles were fabricated on silicon wafers using standard photolithographic techniques. From this silicon master, complementary polydimethylsiloxane (PDMS) replicas were prepared using soft lithography method developed by Whitesides and coworkers<sup>12</sup> and used as stamps in subsequent microcontact printing steps to form patterns of poly (OEGMA-co-MA) copolymer directly on cell culture dishes. Patterned dishes were sterilized under UV for 12 hours before cells were plated

Rac1, RhoA and Cdc42 constitutively active mutants (Rac1L61, RhoA<sup>L63</sup>, and Cdc42L61) and dominantly negative Cdc42N17 were provided by Dr. Yi Zheng (Cincinnati Childrens hospital). Mutants were generated by site-directed mutagenesis based on oligonucleotide-mediated PCR.<sup>13,14</sup> Constitutive active and dominant negative mutants of Rac1, RhoA and Cdc42 (NIH 3T3 fibroblasts) were cultured in Opti-MEM<sup>®</sup> media (w/o phenol red) supplemented with 10% fetal bovine serum and 25mM hepes (All purchased from Invitrogen formerly Gibco). All mutants except CA-NIH3T3-Rac1 were grown by selection with G418 (350 µg/ml). Cell cultures were thermostated using a stage-mounted heater equipped with a temperature controller (OMEGA technologies, Stamford, CT). Patterned cells (500 cells/mL) were supplemented with media containing human PDGF (5 ng/mL) and HEPES buffer (N-(2-hydroxyethyl)-piperazine- N'-2-ethanesulfonic acid; 50 mM) 30 min prior to time-lapse imaging. Phase-contrast images were recorded each hour for the timelapse figures.

Only single cells confined within single islands were considered for analysis. Cells initially spanning more than one island were not included in the analysis. Cells were considered to have “hopped” when their nuclei and 90% of their cell area has moved from one island to another. The 99% confidence intervals of the average speed of motile cells were calculated based on the standard deviation of data collected from at least 100 hopping events and a minimum population of 30 motile cells.

Cells were fixed with 3.7 % paraformaldehyde for 10 minutes, washed in phosphate buffered saline, and then permeabilized with 0.2 % Triton X100 for 5 minutes. Samples were then rinsed with PBS and incubated with Alexa 594-phalloidin, Alexa 488 conjugated anti-Golgin-97 (human) and DAPI to stain for F-actin, Golgi apparatus and nuclei respectively. Images of the patterned cells were acquired using a Nikon TE-2000 inverted microscope with Metamorph software (Ver 6.0r4, Universal Imaging, Westchester, PA)

Golgi polarization of cells patterned over micropatterns was quantified by the fraction of Golgi apparatus in front (r1), side (r2), and rear of their nuclei as shown in Figure 3B. For each cell nuclei, the localization of Golgi within these regions was quantified by measuring the projected area of Golgi apparatus in each region and normalizing with the total projected area of Golgi apparatus around the nucleus. Golgi location within a cell migrating along the array can depend upon the local position of nucleus within a teardrop shape. We further divided the teardrop shape into two regions R1 and R2 and collected data on Golgi localization separately for cells whose nuclei lie exclusively within these regions. Cells whose nucleus reside partly in both R1 and R2 regions were excluded from the analysis.

## Results and Discussion

On non-patterned substrates, cells typically exhibit a polarized morphology with a broader front and narrower rear, and can migrate directionally over a short distance. However, this transient geometry cannot be sustained and cells exhibit random walk behaviors on nonpatterned surfaces. To explore whether arrays of micropatterns can steer cell migration based on morphological polarization alone, we designed arrays of adhesive islands composed of individual teardrops (Figure 1). Each micropattern has an area of  $1000 \mu\text{m}^2$  which is the spreading area of cells exhibiting the fastest rate of migration on non-patterned culture dishes. The gap distance between islands was set to  $3.5 \mu\text{m}$ , which is sufficiently far to confine cells to the islands temporarily but close enough for extended lamellipodia to reach across onto adjacent islands. This gap distance is also shorter than the persistent length of randomly migrating cells. If cells can retain the directional bias set by the asymmetric islands as they traverse between islands, then it may be feasible to direct their migration using microarrays to amplify this natural directional persistence (MANDIP). On these microarrays, NIH3T3 fibroblasts indeed migrate preferentially from the blunt end of the teardrop shapes (Figure 2) leading to continuous movement in the clockwise direction. The two cells shown on the array of teardrop micropatterns move simultaneously. Among 71 observed hops, 69 were in the clockwise direction and only 2 were in the counterclockwise direction, with an average of  $3.3 \pm 1.1$  hours between hops (Table 1).

Golgi apparatus is known to localize preferentially in front of the nucleus of migrating cells.<sup>15</sup> The position of the Golgi apparatus relative to the cell nucleus is characteristic of cell polarity. Cells migrating on the tear drop micropatterns intermittently adopt shapes conforming to the teardrops as they rearrange their cytoskeleton and morphology to migrate. We thus quantified Golgi localization to examine the polarity of cells as they travel on the microarrays. 3T3 fibroblasts, migrating on the teardrop pattern, localize their Golgi towards the blunt end of the teardrops (Figure 3A). Cells migrating along the path and direction set by the microarray can be broadly classified into two groups. One group wherein the cell body is mostly confined to one teardrop island, and a second group wherein the cell body spans two teardrops. To test whether the polarization induced by the geometry of the teardrop is maintained as cells traverse across two adhesive islands, the localization of Golgi apparatus relative to the cell nucleus for these two groups of cells were compared. Dividing the teardrops into blunt (R1) and tip (R2) regions, the nucleus of the first group of cells largely confined to a single teardrop is expected and observed to be mostly confined to the blunt half (R1). Likewise, for the second group of cells that span two teardrops, the nucleus is more likely to be in the tip section (R2). The localization of Golgi apparatus around each cell nucleus was quantified using the schematic shown in Figure 3B. The area of observed Golgi in regions: r1 (front), r2 (sides) and r3 (rear) defined by the two lines intersecting at the nucleus, indicated by the ellipse, were measured. The Golgi apparatus of cells patterned on the teardrop islands are localized mostly in region r1 for both groups of cells. This indicates that the cells remain polarized even as they cross the gap between two islands,

thereby enabling microarray amplification of their natural directional persistence (MANDIP).

The establishment of cell polarity and thus directional motion have been shown to be regulated by an extensive cross talk between various integrins and Rho family of small guanosine triphosphate binding proteins (RhoGTPases). GTPases are the molecular switches that use a simple biochemical strategy to control complex cellular processes. They usually cycle between active GTP and inactive GDP conformational states. Among the several hundred GTPases, Ras superfamily of GTPases including Rac, Rho, and Cdc42 are considered the master regulators of cell polarity and migration.<sup>1,16</sup> Rac activation has been shown to initiate direction extension of lamellipodia<sup>17</sup> and recruit integrins to the edge of the protrusion.<sup>18</sup> Activation of Rho within a cell is associated with the increased actomyosin based tension by signaling through its downstream effector Rho kinase.<sup>19</sup> Over expression of Rho has been shown to increase contractile tension which results in formation of numerous actin bundles and associated mature focal contacts<sup>20–23</sup> and decreases the rate of cytoskeleton reorganizations.<sup>24</sup> In contrast, inhibition of Rho activities by specific genetic constructs or by selective inhibitors leads to disassembly of actin bundles and transformation of focal contacts into small focal complexes. Cdc42 plays an important role in the control of cell polarity. Cdc42 induces formation of numerous filopodia and disrupts the directional motion.<sup>25</sup> Primary fibroblasts expressing dominant negative Cdc42 showed 50% reduction of closure of wound in an *in vitro* wound closure assay.

To investigate whether Rac1, RhoA, and Cdc42 would alter the shape guided polarization and thus migration, we altered the expression levels of these molecules by using adenovirus to express constitutively active Rac1, RhoA, and Cdc42. Patterning NIH3T3 fibroblasts and their constitutively active mutants of Rac1, RhoA, and Cdc42 along with dominant negative mutant of Cdc42 over the teardrop array (Figure 4), we observed that all cell types move preferentially from the blunt end of the teardrop shape to the tip of the neighboring island. For constitutively active Rac1, the figure shows two cells migrating on the array with nearly equal rate. The clockwise directional migration is most consistent for unmodified NIH 3T3 cells with 97% compliance and least consistent for dominant negative Cdc42 cells with 83% compliance (Table 1). Cells that express constitutively activated RhoA migrate at the highest speed with average time between hops of  $1.9 \pm 0.9$  hours and dominant negative mutant Cdc42 were observed to be slowest. These results show that controlling cell shape to cause intermittent morphological polarization of cells can be used to guide directional migration and intracellular signals involved in lamellipodia extension (Rac1), contractility (RhoA), and cell polarity (Cdc42) affect the speed of cell migration on MANDIP microarrays.

Cells with constitutively activated RhoA migrated at nearly double the speed of wild type cells. This suggests that the key step limiting the speed of cell migration on the arrays is the disassembly of adhesions and retraction of the rear. Constitutively activated Rac1 showed preferential migration with the blunt end of the teardrop being the leading edge. The migration speed on the micropatterns is slightly slower compared to the wild type. This indicates that actin polymerization and membrane protrusions, induced by Rac1 activation,<sup>16</sup> are not limiting steps for cell migration for a gap distance of 3.5  $\mu\text{m}$ . The slower speed of migration of Rac1 activated cells can be attributed to suppressed Rho activity as Rac and Rho activation has been shown to be mutually antagonistic,<sup>26</sup> each leading to the deactivation of the other.

Interestingly, both inhibition and activation of Cdc42 lead to reduced migration speed to nearly half of the wild type cells and maintained the direction of migration from the broad end. On non-patterned substrates, inhibiting Cdc42 leads to random protrusion and disrupt the directional cell migration in chemotaxis or wound healing assays.<sup>27</sup> This is the first

example showing cells with dominant negative Cdc42 migrating directionally on preset path. In this case, where a key molecular regulator of cell polarity is absent, the cell polarity and migration of direction is set by the external environment, i.e., cell shape control.

## Conclusions

A new approach has been demonstrated for directing cell movement along preset paths and directions on microarrays of asymmetric islands. Earlier, we reported that cell migration can be directed by limiting access to neighboring adhesive islands from only one end of the teardrop-shaped islands.<sup>9</sup> This study shows that cells can be steered to migrate almost exclusively in one preset direction even when adhesive islands are available on both ends. The asymmetry of the cell shape, as intermittently imposed by the islands, is retained as cells traverse between islands, and enables microarray amplification of natural directional persistence (MANDIP). The observed directional bias is consistent with earlier studies which showed that teardrop shaped cells, released from confinement, move from their blunt ends.<sup>28</sup> This suggests that the global morphology of the cell determines cell polarization. For practical applications, MANDIP is a convenient gradient-free alternative to haptotaxis (ECM gradient)<sup>29</sup>, durotaxis (substrate stiffness)<sup>30,31</sup> or mechanotaxis<sup>32</sup> and can be used to guide the assembly of cells into complex structures with microscale precision over unlimited distances. MANDIP microarrays may also facilitate the examination of molecular pathways that are important to cell polarity and motility.

## Acknowledgments

This work was supported by the National Institutes of Health (award number R01EB010043) and the National Science Foundation (CBET0928219). We thank Dr. Yi Zheng's laboratory for providing the constitutively active and dominant negative fibroblasts.

## References

1. Ridley AJ, Schwartz MA, Burridge K, Firtel RA, Ginsberg MH, Borisy G, Parsons JT, Horwitz AR. *Science*. 2003; 302:1704. [PubMed: 14657486]
2. Small JV, Herzog M, Anderson KJ. *J Cell Bio*. 1995; 129:1275. [PubMed: 7775574]
3. Inoue S, Tilney LG. *J Cell Bio*. 1982; 93:812–819. [PubMed: 6811599]
4. Huxley HE. *Nature*. 1973; 243:445. [PubMed: 4275580]
5. Bray D, White JG. *Science*. 1988; 239:883. [PubMed: 3277283]
6. Grebecki A. *Int Rev Cytol*. 1994; 148:148.
7. Parker KK, Brock AL, Brangwynne C, Mannix RJ, Wang N, Ostuni E, Geisse NA, Adams JC, Whitesides GM, Ingber DE. *FASEB J*. 2002; 16:1195. [PubMed: 12153987]
8. Brock A, Chang E, Ho CC, LeDuc P, Jiang XY, Whitesides GM, Ingber DE. *Langmuir*. 2003; 19:1611. [PubMed: 14674434]
9. Kumar G, Ho CC, Co CC. *Adv Mater*. 2007; 19:1084.
10. Kushiro K, Chang S, Asthagiri AR. *Adv Mater*. 2010; 22:4516. [PubMed: 20818616]
11. Kumar G, Wang YC, Co CC, Ho CC. *Langmuir*. 2003; 19:10550.
12. Singhvi R, Kumar A, Lopez GP, Stephanopoulos GN, Wang DI, Whitesides GM, Ingber DE. *Science*. 1994; 264:696. [PubMed: 8171320]
13. Li R, Debrececi B, Jia BQ, Gao Y, Tigyi G, Zheng Y. *J Bio Chem*. 1999; 274:29648. [PubMed: 10514434]
14. Zindy F, Eischen CM, Randle DH, Kamijo T, Cleveland JL, Sherr CJ, Roussel MF. *Genes Dev*. 1998; 12:2424. [PubMed: 9694806]
15. Nobes CD, Hall A. *J Cell Bio*. 1999; 144:1235. [PubMed: 10087266]
16. Ridley A. *J Cell Sci*. 2001; 114:2713. [PubMed: 11683406]
17. Nobes CD, Hall A. *Cell*. 1995; 81:53. [PubMed: 7536630]

18. Schwartz MA, Shattil SJ. Trends Bio Sci. 2000; 25:388.
19. Watanabe N, Kato T, Fujita A, Ishizaki T, Narumiya S. Nat Cell Bio. 1999; 1:136. [PubMed: 10559899]
20. Kaibuchi K, Kuroda S, Amano M. Annu Rev Biochem. 1999; 68:459. [PubMed: 10872457]
21. Amano M, Chihara K, Kimura K, Fukata Y, Nakamura N, Matsuura Y, Kaibuchi K. Science. 1997; 275:1308. [PubMed: 9036856]
22. Kimura K, Ito M, Amano M, Chihara K, Fukata Y, Nakafuku M, Yamamori B, Feng JH, Nakano T, Okawa K, Iwamatsu A, Kaibuchi K. Science. 1996; 273:245. [PubMed: 8662509]
23. Rao PV, Deng PF, Kumar J, Epstein DL. Invest Ophthalmol Vis Sci. 2001; 42:1029. [PubMed: 11274082]
24. Geiger B, Bershadsky A. Cell. 2002; 110:139. [PubMed: 12150922]
25. Etienne-Manneville S, Hall A. Nature. 2002; 420:629. [PubMed: 12478284]
26. Evers EE, Zondag GCM, Malliri A, Price LS, ten Klooster JP, van der Kammen RA, Collard JG. Euro J Cancer. 2000; 36:1269.
27. Etienne-Manneville S, Hall A. Cell. 2001; 106:489. [PubMed: 11525734]
28. Jiang X, Bruzewicz DA, Wong AP, Piel M, Whitesides GM. Proc Natl Acad Sci USA. 2005; 102:975. [PubMed: 15653772]
29. Rhoads DS, Guan JL. Exp Cell Res. 2007; 313:3859. [PubMed: 17640633]
30. Lo C, Wang H, Dembo M, Wang Y. Biophys J. 2000; 79:144. [PubMed: 10866943]
31. Reinhart-King AA, Dembo M, Hammer DA. Biophys J. 2008; 95:6044. [PubMed: 18775964]
32. Lin XF, Helmke BP. Biophys J. 2008; 95:3066. [PubMed: 18586851]

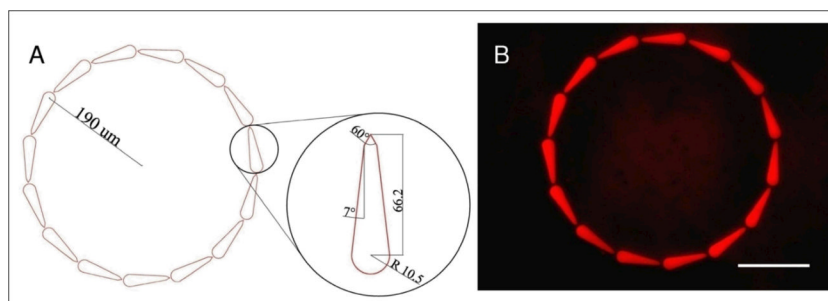


**Figure 1. Steering cell migration using MANDIP microarrays**

(A) Geometry ( $\mu\text{m}$ ) of teardrop array. (B) Fluorescence micrographs showing selective adsorption of Texas Red conjugated BSA on the micropatterns. The background regions were printed with cell and protein resistant poly(OEGMA-co-MA). Scale bar: 100  $\mu\text{m}$ .

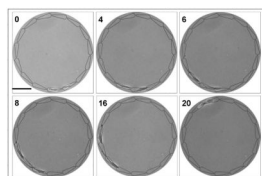


**Figure 2. Continuous directional migration of NIH3T3 cell over MANDIP arrays of teardrop islands**

Time-lapse phase contrast images (in hours) show the continuous directional migration of cells. Scale bar: 100 $\mu$ m.

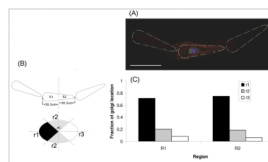


**Figure 3. Teardrop micropatterns polarize cells with the blunt end in front**

(A) Fluorescence micrograph of a single migrating NIH3T3 fibroblast on a teardrop microarray. The cell is stained for actin filaments (red), Golgi apparatus (green) and nucleus (blue). (B) Schematic for quantifying the location of Golgi apparatus. Dotted lines divide teardrop into region R1 and R2 to define the position of nucleus on the teardrop pattern. The surrounding region around each nucleus is divided into three regions r1, r2 and r3. The fraction of Golgi apparatus localized in these regions was measured separately for cells with nucleus located in the R1 (blunt end, representing cells on one teardrop) and R2 (tip end, representing cells span two teardrops) regions. (C) Fraction localization of Golgi apparatus around the nucleus of migrating cells. Scale bar: 50 $\mu$ m.

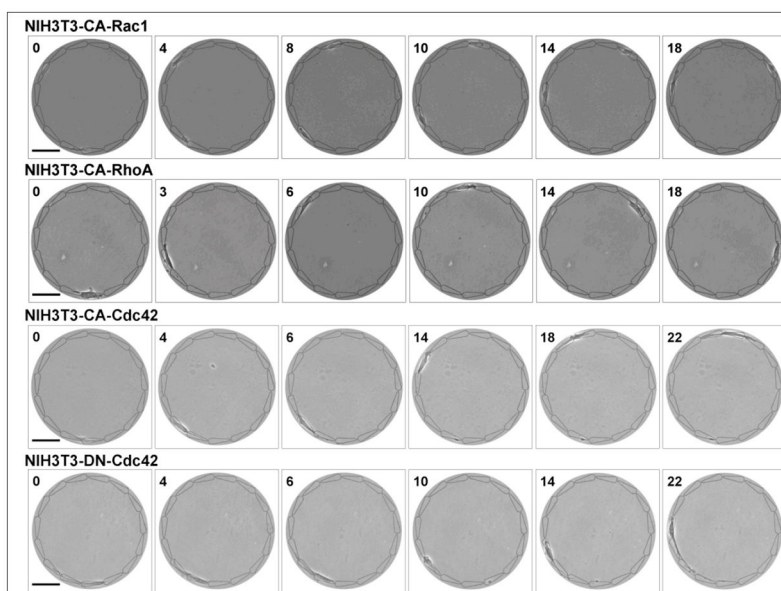


**Figure 4. Continuous directional migration of constitutively active and dominant negative mutants of NIH3T3 fibroblasts**  
Time-lapse phase contrast images (in hours) show the continuous directional migration of cells. Rho activated cells are fastest and dominant negative Cdc42 cells are slowest. Scale bars: 100 $\mu$ m.

**Table 1**

Migration direction and speed of wild-type and mutants of NIH 3T3 fibroblasts.

Cell Type	# Observed Migrations		Average time for single "hop" (hrs)
	CW	CCW	
NIH 3T3	69	2	$3.27 \pm 1.12$
NIH 3T3-CA-Rac1	53	9	$4.87 \pm 1.91$
NIH 3T3-CA-Rho	105	13	$1.86 \pm 0.89$
NIH 3T3-CA-cdc42	89	7	$6.09 \pm 1.46$
NIH 3T3-DN-cdc42	59	12	$6.80 \pm 2.03$